This is a repository copy of *Fundamental study of emulsions stabilized by soft and rigid particles*.

White Rose Research Online URL for this paper:
http://eprints.whiterose.ac.uk/85203/

Version: Accepted Version

Article:

Fundamental study of emulsions stabilized by soft and rigid particles

Zifu Li,[1] David Harbottle,[1,2] Erica Pensini,[1] To Ngai,[3] Walter Richtering,[4] Zhenghe Xu[1,5*]

1, Department of Chemical and Materials Engineering, University of Alberta, Edmonton, Alberta T6G 2V4, Canada

2, School of Chemical and Process Engineering, University of Leeds, Leeds, LS2 9JT, UK

3, Department of Chemistry, the Chinese University of Hong Kong, Shatin, N. T., Hong Kong

4, Institute of Physical Chemistry, RWTH Aachen University, Landoltweg 2, D-52056 Aachen, Germany

5, Institute of Nuclear and New Energy Technology, Tsinghua University, Beijing 100084, China

[*] To whom correspondence should be addressed.

Phone: 1-780-492-7667; Fax: 1-780-492-2881; Email: zhenghe.xu@ualberta.ca

Abstract

Two distinct uniform hybrid particles, with similar hydrodynamic diameters and comparable zeta potentials, were prepared by copolymerizing N-isopropyl acrylamide (NIPAM) and styrene. These particles differed in their styrene to NIPAM (S/N) ratios of 1 and 8, and were referred to as S/N 1 and S/N 8. Particle S/N 1 exhibited typical behavior of soft particles, i.e., the particles shrank in bulk aqueous solutions when the temperature was increased. As a result, S/N 1 particles were interfacially active. In contrast, particle S/N 8 appeared to be rigid in response to temperature changes. In this case, the particles showed negligible interfacial activity. Interfacial shear rheology tests revealed the increased rigidity of the particle-stabilized film formed at the heptane-water interface by S/N 1 than S/N 8 particles. As a result, S/N 1 particles were shown to be better emulsion stabilizers and emulsify a larger amount of heptane compared to S/N 8 particles. The current investigation confirmed a better performance of emulsion stabilization by soft particles (S/N 1) than by rigid particles (S/N 8), reinforcing the importance of controlling softness or deformability of particles for the purpose of stabilizing emulsions.

Keywords: soft and rigid particles, rheology, emulsion stability

1. Introduction

Particle-stabilized emulsions, which are also known as Pickering[1] emulsions, were described a century ago. The stability of particle-stabilized emulsions has been attributed to steric repulsion between the layers of particles at the oil-water interface.[2] There has been a renewed interest in particle-stabilized emulsions for several desirable reasons.[2-3] First, understanding the role of particles at the oil-water interface is of paramount importance for a number of practical applications[2] including the production of food,[4] cosmetics and coatings,[5] and petroleum processing.[6] Second, particles trapped at the oil-water interface are an excellent experimental and theoretical model for the study of phase behaviors in two-dimensional[7] and geometrically frustrated systems.[8] Third, particle-stabilized emulsions provide a simple and novel template for the production of various functional materials.[9]

From an application point of view, particle-stabilized emulsions with stimuli-responsive properties are highly desirable.[10] Such emulsions can be stabilized and subsequently destabilized on demand via tuning the external conditions, such as pH, temperature, and UV radiation.[11] For example, to resolve the problems encountered in two-phase enzyme-catalyzed reactions, Wiese et al.[12] presented a conceptually novel approach using poly(N-isopropyl acrylamide) (PNIPAM)-based microgel-stabilized smart emulsions for biocatalysis. Many substrates of interest for biocatalytic reactions are organic soluble, while enzymes usually preferentially reside in the aqueous environment. Therefore, enzyme catalyzed biocatalytic reactions are often carried out in biphasic aqueous-organic reaction mixtures to achieve high substrate concentration and high productivity.[13] Moreover, enzymes structures and flexibility might be affected by the organic-aqueous interface, thus leading to reduced enzyme activity and selectivity. PNIPAM-based microgel-stabilized smart emulsions not only stabilize the enzyme against denaturation at the oil-

water interface but also increase the area between organic and aqueous phases, ensuring the success of these enzyme-catalyzed reactions. Furthermore, PNIPAM-based microgel-stabilized smart emulsions can be broken after stirring for 10 min at 50℃, allowing for simple product separation as well as recycling of enzymes and microgels.[12]

The use of PNIPAM-based microgels as stimuli-responsive emulsions stabilizers is well documented and generated substantial research interest over the last few years.[14] However, the mechanisms through which PNIPAM-based microgels can stabilize and destabilize emulsions are far from well understood.[15] PNIPAM-based microgels are colloidal particles with chemically crosslinked three-dimensional polymer networks.[16] Such microgels are soft particles and have both colloid and polymer characters,[16] which are inherently different from rigid particles, such as polystyrene latexes or silica particles.[17] The soft microgel particles swell in water, and are well-known for their volume phase transition temperature (VPTT) around 32℃.[18] For conventional rigid Pickering stabilizers, it is well documented that the key parameter for controlling emulsion type and stability is the wettability of particles measured by contact angle of the particles at the oil-water interface.[19] This key parameter is hardly applicable for microgels, because microgels can easily deform[20] at the oil-water interface, protruding only slightly into the oil phase.[15, 21] The stability of microgels-stabilized emulsions has been largely attributed to the deformability of PNIPAM-based microgels.[20, 22] However, the rationale regarding microgels deformability and emulsion stability is not yet understood, and calls for further investigation.[23] The goal of the work presented in this paper is to elucidate the mechanisms on how particle deformability correlates to emulsion stability.

2. Materials and Methods

2.1 Materials and Chemicals

N-isopropylacrylamide (NIPAM, ≥99%, Sigma), N, N'-methylenebis-(acrylamide) (BA, 99%, Sigma), potassium persulfate (KPS, Merck), styrene (≥99%, Sigma) and n-heptane (HPLC grade, Sigma) were used as received without further purification. Milli-Q water with a resistivity of 18.2 MΩ·cm was used in all experiments.

2.2 Preparation of particles

Two different particles were prepared with varied styrene to NIPAM (S/N) ratios. Namely S/N 1 (styrene to NIPAM weight ratio equal to 1) and S/N 8 (styrene to NIPAM weight ratio equal to 8), were prepared and used for the current investigation.[24] These particles were crosslinked with BA.[18] Styrene (4.50 g), BA (0.15 g), and NIPAM (4.50 g for S/N 1 and 0.56 g for S/N 8) were added into 500 mL of deionized water in a 1000 mL three-neck reactor fitted with nitrogen bubbling inlet and outlet, equipped with a reflux condenser and a mechanical stir. After stirring the solution for 40 min at 70 ℃ under nitrogen bubbling, the polymerization was initiated by adding potassium persulfate ($K_2S_2O_8$, KPS, 0.15 g) dissolved in 10 mL of deionized water. The reaction was conducted at 70 °C for 7 hrs and then cooled to 25 ℃. The mixture was subsequently filtered through glass wool to remove large aggregates and further purified by repetitive centrifugation at 10000g for 1 hr and dispersion in deionized water for five times. The purified particles were re-dispersed in deionized water and the particle weight percentage in the resultant solution was determined by weighing the residual weight after evaporation of water in vacuum oven at 60 ℃ overnight.

2.3 Zeta potential analyzer using Phase Analysis Light Scattering (Zeta PALS)

The electrophoretic mobility, μ_e, of these particles was measured using a zeta potential analyzer (Zeta PALS, Brookhaven) in 10 mM NaCl aqueous solutions at 25℃. In the zeta potential measurement, charged particles in a dilute suspension (10^{-5} g of particles in 1 mL solution) moved between two oppositely charged electrodes. The fundamental measurement was the velocity of these charged particles under a given electric field.[25] The velocity was measured using dynamic laser light scattering (with a laser wavelength at λ=660 nm). Ten measurements were collected to calculate the mean values and standard deviations.

2.4 Dynamic Light Scattering (DLS)

DLS measurements of S/N 1 and S/N 8 particles (10^{-5} g/mL) were carried out at a scattering angle of 90° using an ALV 5022 laser light-scattering (LLS) instrument equipped with a cylindrical He−Ne laser (model 1145p-3083; output power = 22 mW at wavelength λ = 632.8 nm) in combination with an ALV SP-86 digital correlator of a sampling time ranging from 25 ns to 40 ms. The temperature of the experiments was controlled within ± 0.02 °C by a thermostat. The samples were left to equilibrate for at least half an hour after the temperature had been changed. Every single measurement (at specific temperature) was completed in 5 min and repeated at least three times. The hydrodynamic radius was obtained from the measured diffusion coefficient D via the Stokes-Einstein equation, R_h = k_BT/($6\pi\eta D$), where η, k_B, and T are the solvent viscosity, the Boltzmann constant, and the absolute temperature, respectively.[26]

2.5 Scanning Electron Microscope (SEM) imaging

SEM images were obtained using a Hitachi S-2700 scanning electron microscope equipped with a Princeton gamma tech IMX digital imaging system. The accelerating voltage used was 10 KV and the magnification was 15000×. For SEM sample preparation, one drop of S/N 1 or S/N 8 dilute suspension (5×10^{-4} g/mL) was pipetted on a clean silica wafer and dried in air at 25 ℃ overnight.

2.6 Pendant Drop Tensiometer

The principle of the pendant drop tensiometer measurement is detailed elsewhere.[27] For Drop Shape Analysis (DSA) the instrument records a sequence of droplet images, with the droplet edge fitted to theoretical curves to obtain the best fitting interfacial tension. The interfacial tension was measured using DSA100 (Krüss GmbH, Hamburg, Germany). Droplet volume V, droplet interfacial area A, and interfacial tension γ can be measured. To maintain a constant temperature, the cuvette was placed in a chamber and the temperature was controlled with an external cryostat. The study of particle interfacial activity was carried out at the heptane-water interface in the presence of S/N 1 or S/N 8 particles. The density difference between water and heptane is 0.314 g/mL. For dilute particle solutions, the density increase is negligible, thus the density difference between water and heptane remains applicable. After droplet creation, the droplet shape evolves as particles adsorb to the interface. The evolution in droplet shape can be interpreted to determine the interfacial tension and subsequently the interfacial pressure. The interfacial activity of the particles can then be determined from the evolution of the heptane-water interfacial pressure.[28] Refer to the supporting information for more details.

2.7 Preparation of particle-stabilized emulsions and bottle tests

S/N 1 and S/N 8 particle-stabilized emulsions were prepared with a fixed heptane to water volume ratio of 1:4. S/N 1 or S/N 8 particles were first dispersed in water to a particle concentration of 1.25×10^{-3} g/mL. Heptane-in-water emulsions were prepared by the following three methods: 1] homogenizing at 15000 rpm for 1 min; 2] handshaking for 1 min; and 3] self-assembly method by ejecting heptane droplets into water containing the microgel particles using a 1 mL micropipette. Emulsions were prepared using 1 mL heptane and 4 mL particles solution, to obtain a total emulsion volume of 5 mL. Note, to determine the encapsulated heptane volume in each emulsion, perylene dye was purposely added (1.5×10^{-5} g/mL) to the heptane.

Following emulsion preparation, 3 mL of heptane was further added on top of the formed emulsion. With the perylene dye in the emulsified heptane, the encapsulated heptane volume can be determined by measuring the perylene dye concentration in the free heptane phase, using UV-Vis-NIR spectrophotometer (Shimadzu UV-3600). The emulsion droplets were imaged 24 hrs after preparation using a Carl Zeiss Axioskop 40 Pol optical microscope at 20× magnification to obtain the emulsion droplets mean size and standard errors of emulsion droplets by analyzing 60 emulsion droplets.

2.8 Interfacial Shear Rheometer (ISR)

Interfacial shear rheology measurements were conducted using a stress-controlled rheometer (TA Instruments AR-G2), equipped with double wall ring (DWR) geometry.[29] 19.2 mL S/N 1 or S/N 8 particle dispersion (5×10^{-4} g/mL) was added to a PTFE circular trough. The flamed DWR geometry was then positioned at the air- water interface prior to gently pipetting 15 mL HPLC grade heptane to form the top phase. After introducing the two liquid phases, the interfacial film was left to age for 40 min to allow the microgel particles to adsorb at the heptane-water interface.

Strain sweep experiments were carried out in an oscillation mode at a frequency of 0.3 Hz.[29] More details of this technique and device can be found elsewhere.[30]

3. Results and Discussion

As shown in Table 1, particles S/N 1 and S/N 8 had similar surface charges and hydrodynamic diameters in 10 mM NaCl electrolyte aqueous solution at 25 ℃. The electrophoretic mobility (μ_e) was $-4.06 \pm 0.08 \times 10^{-8}\ m^2 V^{-1} s^{-1}$ for S/N 1 and $-4.30 \pm 0.07 \times 10^{-8}\ m^2 V^{-1} s^{-1}$ for S/N 8 particles. Considering that the diameters of S/N 1 and S/N 8 particles were around 200 nm and that the Debye length was 3 nm in 10 mM NaCl solution, the Smoluchowski model can be applied to calculate the zeta potential values from the measured electrophoretic mobility.[25] The zeta potential of S/N 1 and S/N 8 particles was calculated to be around -55 mV. This result shows that the negative charge density of S/N 1 and S/N 8 is greater compared to that of PNIPAM microgel particles, with a nominal zeta potential ~-20 mV at a temperature below the VPTT.[18, 28] The significantly more negative charge density of S/N 1 and S/N 8 particles is possibly due to residual sulfate groups, originating from the decomposition of initiator KPS. It is well documented that below the VPTT, PNIPAM particles adopt a core-corona structure.[21, 31] Dangling chains at the periphery can screen the residual sulfate groups, lowering the zeta potential value.[32]

The hydrodynamic diameters of S/N 1 and S/N 8 particles in aqueous solution were ~200 nm, with very narrow distributions, as determined from DLS measurements. SEM images of S/N 1 and S/N 8 particles further showed that they were highly uniform, as shown in Fig. 1. Exposure to air caused a reduction in the microgel particle size, from ~200 nm to ~140 nm, and from ~200 nm to ~190 nm for S/N 1 and S/N 8, respectively.

Table 1. Zeta potential and hydrodynamic diameter of S/N 1 and S/N 8 particles at 25 ℃.

Particles	Zeta potential (mV)	Diameter (nm)
S/N 1	-55±1	202±16
S/N 8	-58±1	200±11
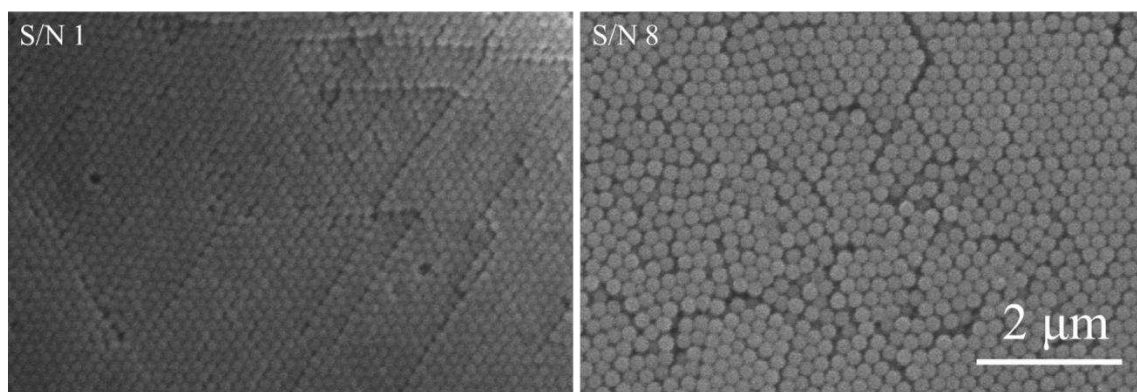
Figure 1. Scanning electron microscope images of S/N 1 and S/N 8 particles. Image scale bar = 2 μm.

Fig. 1 further shows that the boundaries between S/N 1 particles were blurred, whereas the boundaries between S/N 8 particles were clearly defined. The differences in the size change upon exposure to air and in the clarity of the boundaries between particles are ascribed to the particle hardness as a result of different styrene to NIPAM ratios in S/N 1 and S/N 8. It is well known that PNIPAM particles shrink significantly after drying in air and penetrate into each other at high packing densities.[16] Although S/N 1 particles are more negative compared to the zeta potential of PNIPAM particles, they exhibited typical soft PNIPAM particle behaviors, shrinking after drying and blurred boundaries at high packing density.[16] Conversely, S/N 8 particles behaved as rigid particles.
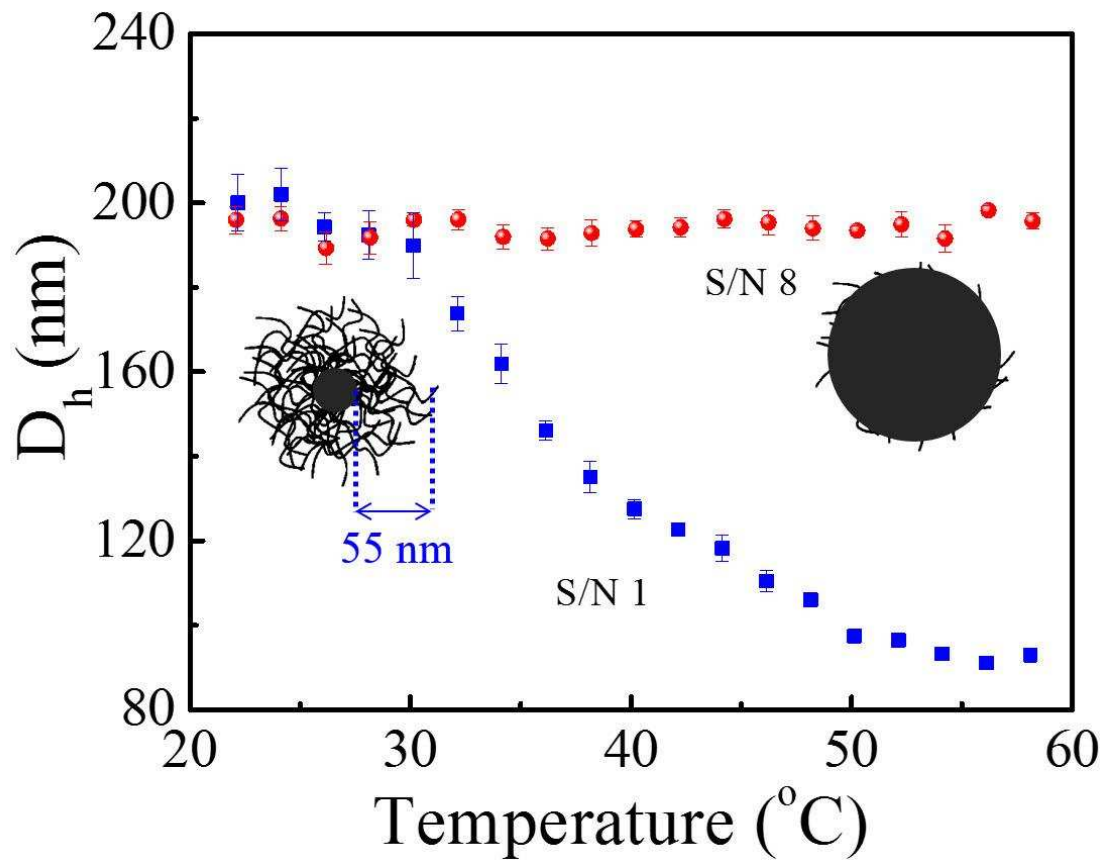
Figure 2. Hydrodynamic diameter (D_h) of S/N 1 and S/N 8 particles as a function of the solution temperature.

Fig. 2 shows a significant difference between S/N 1 and S/N 8 particles in bulk solution in response to a temperature change. S/N 1 particles shrank progressively from 200 nm to 90 nm upon heating from 30 ℃ to 50 ℃, whereas S/N 8 particle size remained unchanged over the same temperature range. This observation is in agreement with previously reported data.[28, 33] In contrast to S/N 8, S/N 1 particles exhibited a thermal responsive property.[24] However, unlike PNIPAM particles which typically exhibit a sharp transition around the VPTT,[16, 18, 28] S/N 1 particles showed a continuous decrease from ∼200 nm to ∼90 nm, with a collapse ratio of ∼2.22 over a temperature change from 30 ℃ to 50 ℃. This difference in transition characteristic is

11

attributed to the addition of styrene to NIPAM.[33] Because PNIPAM is amphiphilic, even at temperatures above PNIPAM's VPTT,[24] S/N 1 particle can be described as a particle with PS-rich dense core and PNIPAM-rich loose shell in water,[28] while S/N 8 particle is PS-rich core with a negligible thin PNIPAM periphery layer at the particle surface, as shown in Fig. 2. This difference in S/N 1 and S/N 8 particles peripheries agrees well with the observed difference in Fig. 1.
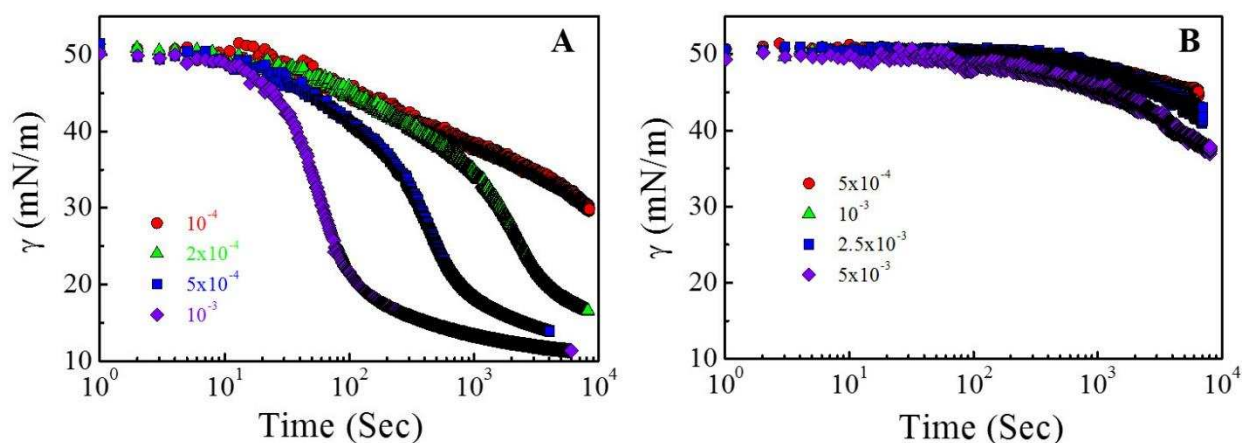
Figure 3. The effect of particle concentrations on the heptane-water interfacial tension γ, A for S/N 1, and B for S/N 8, at 25 ℃. The concentration unit of S/N 1 and S/N 8 is g/mL.

Due to different S/N ratios, S/N 1 particles possessed distinctive softness as compared with S/N 8 particles, resulting in varied properties not only in bulk solution but more importantly at the heptane-water interface. As shown in Fig. 3, S/N 1 particles were more interfacially active than S/N 8 particles. It is worth noting that higher concentrations had been used for S/N 8 particles compared with S/N 1 particles. Clearly, S/N 1 particles prepared to a dispersion concentration of 10^{-3} g/mL, can effectively decrease the heptane-water interfacial tension from 50 mN/m to ~ 10 mN/m after 1000 sec, indicating spontaneous adsorption behavior. Spontaneous adsorption behavior suggests that the adsorption energy barrier is small or even absent for S/N 1 particles.

Such barrier-free adsorption is unique for soft PNIPAM microgel, due to the polymer nature of PNIPAM microgel.[34] It is well documented that both PNIPAM chains[35] and microgels[28] spontaneously adsorb onto oil-water interfaces because of the amphiphilicity of PNIPAM, which includes both hydrophobic isopropyl and hydrophilic amide groups.[36] For S/N 8 particles, also at 10^{-3} g/mL, the heptane-water interfacial tension does not significantly decrease even after 6000 sec. Increasing the particle concentration to 5×10^{-3} g/mL exerts negligible effect on decreasing the heptane-water interfacial tension. These experimental observations suggest there is an energy barrier for S/N 8 particle adsorption onto the heptane-water interface,[37] typical for solid particle adsorption behavior at the oil-water interface.[37-38]

Table 2. Diffusion coefficients in bulk and adsorption coefficients onto the heptane-water interface of S/N 1 and S/N 8 particles, at 25 ℃.

Particles	D_{bulk} ($\mu m^2 \cdot s^{-1}$)	D_{ads} ($\mu m^2 \cdot s^{-1} \cdot mol^2 \cdot g^{-2}$)*
S/N 1	1.78±0.12	$(2.43 \pm 0.08) \times 10^{-7}$
S/N 8	1.80±0.09	$(1.93 \pm 0.13) \times 10^{-9}$

* Note the unit of D_{ads} is different from that of D_{bulk}. For this reason, D_{ads} cannot be directly compared with D_{bulk}. D_{bulk} is experimentally determined by DLS.

To quantify the adsorption behaviors of S/N 1 and S/N 8 particles onto the heptane-water interface and compare their interfacial activities, the data in Fig. 3 were further analyzed according to a diffusion controlled adsorption model derived by Ward and Tordai.[39] The details on the derivation of adsorption coefficient, D_{ads}, using the Ward-Tordai equation are given in the supporting information.[28, 38] It should be noted that D_{ads} describes the adsorption process of the

particles from boundary layer in water near the oil-water interface into the oil-water interface, which is different from the two-dimensional diffusion of the particles in the oil-water interface as reported by Fuller et al[23] and Dai et al[40]. In this study only the initial adsorption stage, when particles first adsorb to the heptane-water interface with low particle coverage,[38] is used for determining D_{ads}. With a low interfacial coverage, particles can freely adsorb to the interface and this adsorption behavior is governed by the excess energy released upon partition of the particles to the interface.[28] The linear relation as shown in Figure S3 verifies that D_{ads} is a constant for a given particle/oil-water interface system as anticipated. As interfacial coverage increases, the adsorbed particles repel new particles from adsorbing to the interface.[38] As a result, particles adsorption to the oil-water interface is reduced. The interaction between the particles at the oil-water interface and adsorbing particles from aqueous solutions makes the Ward-Tordai equation no longer valid, as shown by the deviation from the linear plot in Figures S1 and S2. Table 2 shows that D_{ads} for S/N 1 particles is 126 times greater than that of S/N 8 particles, though both S/N 1 and S/N 8 have similar bulk diffusion coefficients, D_{bulk}. The difference in D_{ads} implies that S/N 1 particles adsorb much faster onto the oil-water interface than S/N 8 particles, due to the fact that there is a 55 nm thick PNIPAM shell in S/N 1 particles but a negligible PNIPAM periphery in S/N 8 particles.

As shown in Fig. 4A-C, S/N 1 particles were identified as the better emulsion stabilizer compared to S/N 8 particles, indicated by the encapsulation of more perylene dye in the emulsion. Note that an additional 3 mL of heptane was added at the emulsion-air interface after emulsion preparation. For emulsions stabilized by S/N 8 particles, the heptane layer appeared blue, indicating little retention of the perylene dye in the emulsion droplets. For S/N 1 particles, it appeared that most of the perylene dye was encapsulated in the emulsion droplets, whose sizes

largely depended on the preparation method, as revealed in Fig. 4D-F. The droplet size for emulsion prepared with S/N 1 particles was 16 ± 6 μm for homogenizer, 18 ± 5 μm for handshaking, and 63 ± 5 μm for self-assembly. With the same emulsification method, the emulsion droplet sizes decreased with increasing S/N 1 particles concentration, as shown in Fig. S4 (ESI†).[20] When emulsions were prepared by homogenizing heptane and S/N 1 particle suspension, the droplet size was 28 ± 5 μm at $1.25 \times 10^{-4} g/mL$, 24 ± 10 μm at $2.5 \times 10^{-4} g/mL$, and 19 ± 9 μm at $5 \times 10^{-4} g/mL$. When emulsions were prepared by handshaking heptane and S/N 1 particle suspension, the droplet size was 34 ± 11 μm at $1.25 \times 10^{-4} g/mL$, 22 ± 6 μm at $2.5 \times 10^{-4} g/mL$, and 21 ± 7 μm at $5 \times 10^{-4} g/mL$.[41]
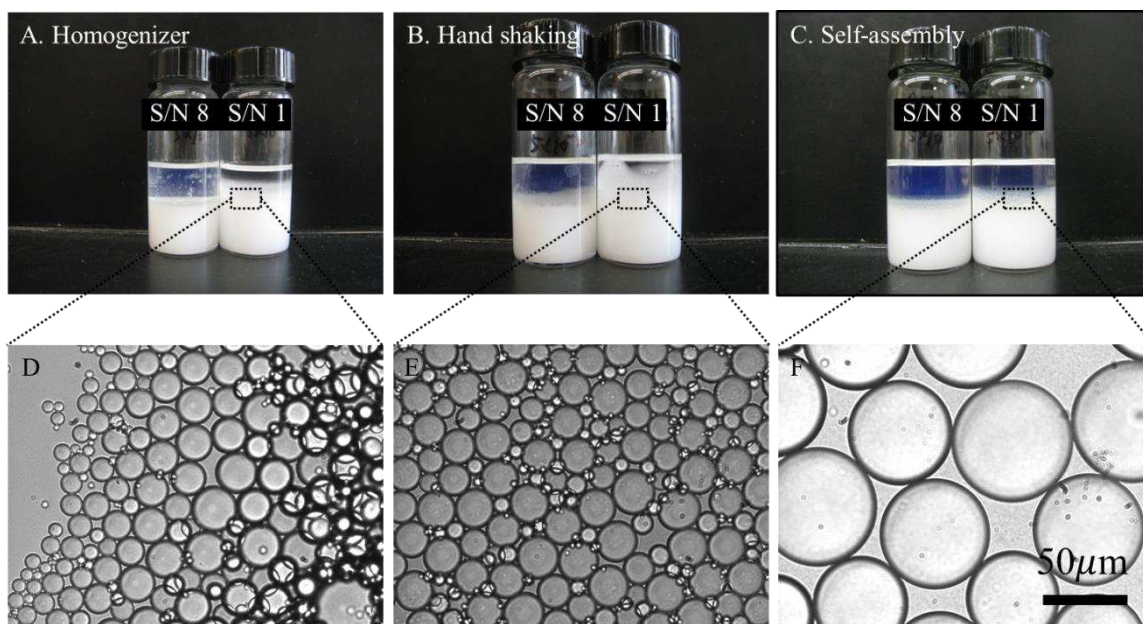
Figure 4. Appearance of (A) homogenizer, (B) handshaking, and (C) self-assembly emulsions stabilized by S/N 1 and S/N 8 particles at 1.25×10^{-3} g/mL, taken by a Canon Digital IXUS 860IS camera 24 hrs after their preparation; optical microscope images of (D) homogenizer, (E) handshaking, and (F) self-assembly emulsions stabilized by S/N 1 particles. Images of D-F, scale bar = 50 μm.

In Fig. 5, the encapsulated heptane (Y-axis) refers to the heptane in the form of stable emulsion droplets. The change in the perylene dye concentration in the free heptane phase was used as a measure of emulsion stability. For the same emulsification method, Fig. 5 reveals that soft S/N 1 particles were always more effective than hard S/N 8 particles at stabilizing the emulsion droplets. Using S/N 1 particles, long term emulsion stability (~90% over 1 month) was observed regardless of the emulsion preparation method; homogenizer or handshaking. This long term stability confirmed that the addition of a bulk oil layer on top of the emulsion did not impact the stability of the prepared emulsions. It confirms that the change in emulsion stability (as measured by the release of perylene dye) was governed by droplet coalescence and not by diffusion of the perylene dye out of the particle-stabilized droplets. For emulsions stabilized by S/N 1 particles, the emulsion stability decreased in the following order: homogenizer = handshaking > self-assembly.
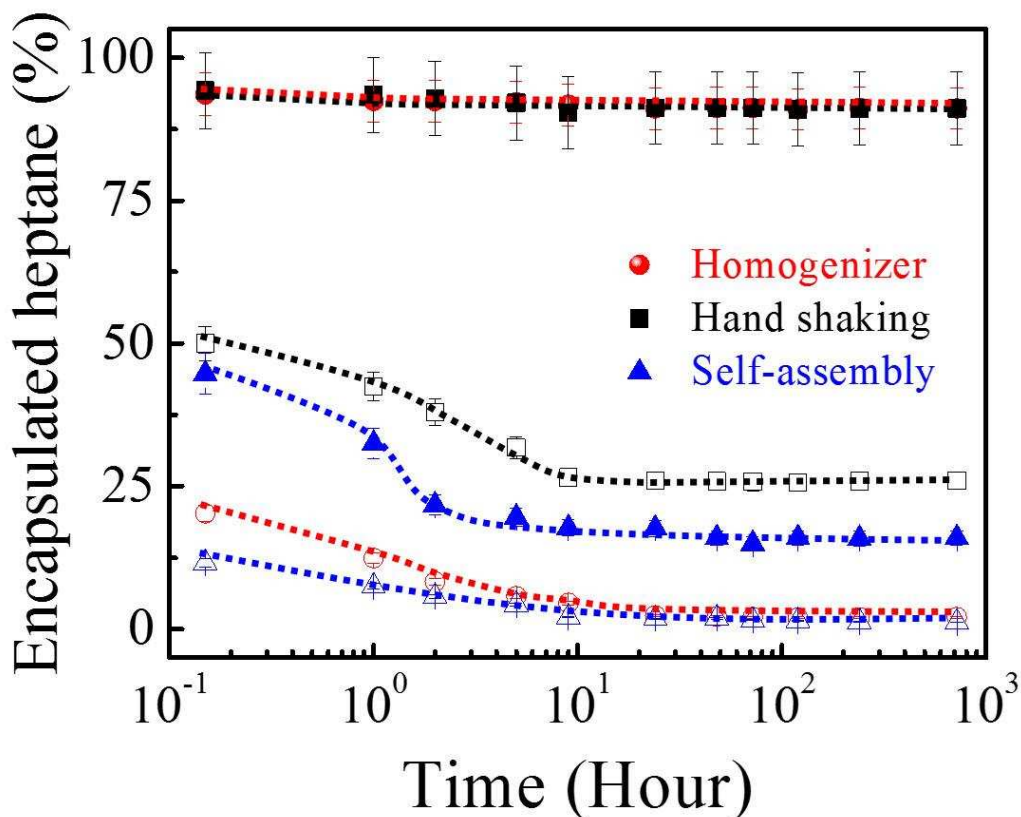
Figure 5. Time dependence encapsulation of heptane in emulsion droplets prepared using S/N 1 and S/N 8 particles (1.25×10^{-3} g/mL): solid symbols for S/N 1 and open symbols for S/N 8.

The significant reduction in emulsion stability by the self-assembly method can be understood from the particle dynamics and the time required for particles to partition at the liquid-liquid interface. The self-assembly method relies on the production of droplets at the needle tip with every drop released within 10 seconds. Such rapid production and release of the droplet does not provide sufficient time for particles to effectively migrate and partition and the liquid-liquid interface. For example, considering the data shown in Fig. 3A, the time required for the oil-water interfacial tension to decrease sharply is greater than 20 s (1×10^{-3} g/mL: $\Delta t \sim 20$ seconds, $\Delta \gamma \sim 2$ mN/m). Due to a low particle surface coverage on droplets, the droplets are not sufficiently stabilized by particles to prevent coalescence.[42] As a result, the emulsion observed is unstable for

17

both particle systems. In this case, particle properties appear to show a negligible effect on emulsion stability. The remaining stable droplets (< 20%) most likely result from drop-drop coalescence which leads to an increase in the interfacial particle concentration as a result of decreasing the overall interfacial area.[43] With a negligible adsorption energy barrier, S/N 1 particles spontaneously adsorb onto the heptane-water interface, as shown in Figure 3. Thus enhanced mixing by handshaking and/or homogenizing increases emulsion stability by rapidly partitioning S/N 1 particles at the heptane-water interface.

For hard S/N 8 particles, the emulsion stability decreases from handshaking to homogenizer and then self-assembly. It should be emphasized that all the emulsions prepared by S/N 8 particles are unstable, encapsulating less than 30% heptane after 1 month testing. These results further verify the presence of an adsorption energy barrier for S/N 8 particles. Hence, the stabilizing potential of the S/N 8 particles is low, even though substantial agitations, handshaking and homogenizing, have been applied to mix S/N 8 particle dispersions with heptane. The slightly higher stability of emulsions prepared by handshaking than by homogenizer could be a result of the difference in energy input during emulsification: lower energy input by handshaking than by mechanical mixing. It is also observed that emulsions formed by handshaking produced larger emulsion droplets as compared with emulsions made by mechanical mixing, as shown in Fig. S6 (ESI†). Since the total number of S/N 8 particles added to the emulsion is the same, a larger volume of oil can be encapsulated in emulsions of larger size droplets for a given oil-water interfacial area covered by S/N 8 particles.[43] For this reason, more oil is encapsulated in emulsions made by handshaking than that by mechanical mixing (homogenizer).

Considering emulsification, Figure 3 clearly demonstrates that S/N 1 particles adsorb faster than S/N 8 particles onto the heptane-water interface, providing partial justification for the difference

in the stability of emulsions. In addition, we know that S/N particles form a monolayer[34] at the oil-water interface, hence, differences in stability associated with hand-shaken and homogenization can be further understood from equilibrium interfacial tension data. For S/N 1 particles, the equilibrium interfacial tension is $\gamma \sim 10$ mN/m. However, for S/N 8 particles, it is difficult to determine the equilibrium interfacial tension from the current data shown in Figure 3. To measure the equilibrium interfacial tension or interfacial pressure for both S/N 1 and S/N 8 particles, the Langmuir trough was used to compress an interfacial layer of particles at the heptane-water interface; experimental details and data are provided in the supporting information. As shown in Figure S7, when the two interfacial films are compressed, both particle monolayers (S/N 1 and S/N 8) reach different interfacial pressures at the maximum compression area. It is also worth noting that the interfacial pressure of S/N 1 particles is always greater than S/N 8 particles at equivalent interfacial areas. In fact, the interfacial pressure for S/N 8 particles at the minimum surface area is lower than that for S/N 1 particles at the maximum surface area. Such behavior demonstrates the difficulty in partitioning, packing and maintaining S/N 8 particles at the oil-water interface, hence, the interfacial films provide less resistance to droplet coalescence. Therefore, when the two particle systems are exposed to the same method of agitation for an equivalent time (1 minute handshaking and/or 1 minute homogenizing), S/N 1 particles would be expected to form a more stable interfacial film which can resist droplet coalescence and hence maintain the encapsulation of a larger volume of heptane for a prolonged period of time, as shown in Figure 5.

To further understand the mechanism that governs the contrasting emulsion droplet stability we considered the shear rheological properties of the S/N 1 and S/N 8 particle-stabilized interfaces.[29] After aging the particle suspension-heptane interface for 40 min, the viscoelastic (G″ viscous, G′

19

elastic) properties were measured by performing a strain sweep at a constant frequency (0.3 Hz). Both interfaces were found to be dominated by an elastic microstructure ($G' > G''$), with the G' and G'' contributions of the interface formed by S/N 1 particles exceeding those formed by S/N 8 particles. For the interfaces stabilized by S/N 1 particles, the breakdown of the solid-like ($G' > G''$) microstructure occurred at a higher strain (~300%) as compared to the interface formed by the S/N 8 particles (~200%). The greater shear elastic stiffness and yield point of the interface formed by S/N 1 particles as compared with the interface formed by S/N 8 particles would support the observed difference in emulsion stabilizing potential.[29] It should be emphasized that the interface in the shear rheological measurement is mostly representative of interfaces encountered in emulsions prepared by self-assembly method, since both interfaces were formed by particle diffusion and adsorption in the absence of any agitation. For such systems the difference in emulsion stability is considerably lower than that observed for the emulsions prepared by homogenizer or handshaking method. Given the observations in Fig. 1-3 and 6, it is highly plausible that deformable S/N 1 particles spontaneously adsorbed and overlapped (or interpenetrated) with adjacent particles to form rigid interfaces, which could withstand the relatively high applied shear force that ultimately result in stable emulsion droplets.[15, 20, 44]
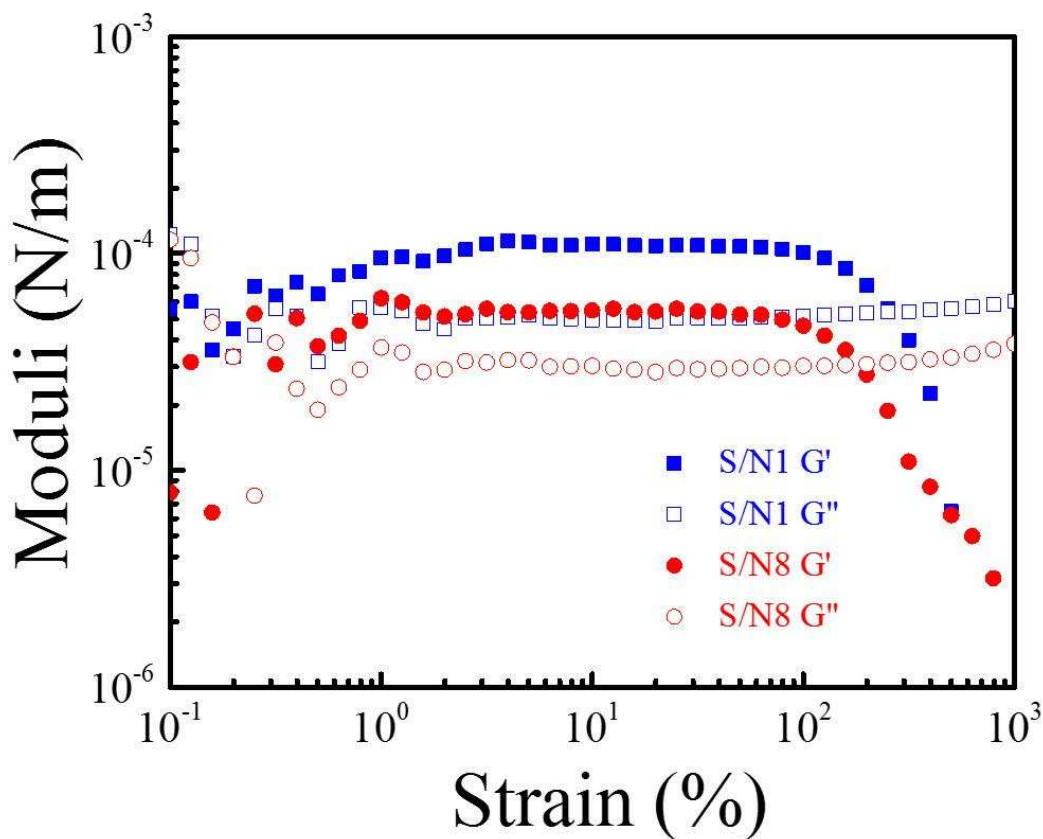
Figure 6. Strain sweep of S/N 1 and S/N 8 particles covered heptane-water interface at applied frequency of 0.3 Hz.

Conclusions

In this study, NIPAM and styrene were copolymerized to prepare two different uniform hybrid particles. Both particles were characterized and used as emulsion stabilizers. Bottle tests demonstrated that soft particles (S/N 1), which incorporated higher amounts of NIPAM, were better emulsion stabilizers as compared with the more rigid particles (S/N 8). For a given particle concentration, soft particles emulsified more heptane as compared to rigid particles and allowed the emulsions to remain stable over longer periods of time. The two particles considered were of similar size and zeta potential in bulk aqueous solutions at 25 ℃, but were composed of different

styrene to NIPAM ratios (1 for S/N 1 and 8 for S/N 8). S/N 1 particles exhibited soft particle behavior in bulk solution, with the particles shrinking upon increasing temperature, and exhibited high interfacial activity at the heptane-water interface. In contrast, S/N 8 particles showed no thermal response in bulk solution and insignificant interfacial activity at the heptane-water interface. Compared with S/N 8 particles, interfaces formed by S/N 1 particles were more rigid under shear and therefore were more effective in stabilizing emulsions. The current study demonstrated that soft particles (S/N 1) were more efficient emulsion stabilizers than rigid particles (S/N 8).

Acknowledgement

References

1.   Pickering, S. U., CXCVI.-Emulsions. Journal of the Chemical Society, Transactions **1907,** 91, 2001-2021.

2.   Binks, B. P.; Horozov, T. S., Colloidal Particles at Liquid Interfaces. RSC: Cambridge, 2006.

3.   Vignati, E.; Piazza, R.; Lockhart, T. P., Pickering emulsions: Interfacial tension, colloidal layer morphology, and trapped-particle motion. Langmuir **2003,** 19 (17), 6650-6656.

4.   Dickinson, E., Hydrocolloids at interfaces and the influence on the properties of dispersed systems. Food Hydrocolloids **2003,** 17 (1), 25-39.

5.   Garbin, V., Colloidal particles: Surfactants with a difference. Physics Today **2013,** 66 (10), 68-69.

6.   Sullivan, A. P.; Kilpatrick, P. K., The effects of inorganic solid particles on water and crude oil emulsion stability. Industrial & Engineering Chemistry Research **2002,** 41 (14), 3389-3404.

7.   Nikolaides, M. G.; Bausch, A. R.; Hsu, M. F.; Dinsmore, A. D.; Brenner, M. P.; Weitz, D. A.; Gay, C., Electric-field-induced capillary attraction between like-charged particles at liquid interfaces. Nature **2002,** 420 (6913), 299-301.

8.   Irvine, W. T. M.; Vitelli, V.; Chaikin, P. M., Pleats in crystals on curved surfaces. Nature **2010,** 468 (7326), 947-951.

9.   Grzelczak, M.; Vermant, J.; Furst, E. M.; Liz-Marzan, L. M., Directed Self-Assembly of Nanoparticles. Acs Nano **2010,** 4 (7), 3591-3605.

10.   Cayre, O. J.; Chagneux, N.; Biggs, S., Stimulus responsive core-shell nanoparticles: synthesis and applications of polymer based aqueous systems. Soft Matter **2011,** 7 (6), 2211-2234.

11.   Jiang, J.; Zhu, Y.; Cui, Z.; Binks, B. P., Switchable Pickering Emulsions Stabilized by Silica Nanoparticles Hydrophobized In Situ with a Switchable Surfactant. Angewandte Chemie-International Edition **2013,** 52 (47), 12373-12376.

12.   Wiese, S.; Spiess, A. C.; Richtering, W., Microgel-Stabilized Smart Emulsions for Biocatalysis. Angewandte Chemie-International Edition **2013,** 52 (2), 576-579.

13.   Vick, J. E.; Schmidt-Dannert, C., Expanding the Enzyme Toolbox for Biocatalysis. Angewandte Chemie-International Edition **2011,** 50 (33), 7476-7478.

14.   Ngai, T.; Behrens, S. H.; Auweter, H., Novel emulsions stabilized by pH and temperature sensitive microgels. Chemical Communications **2005,** (3), 331-333.

15.   Richtering, W., Responsive Emulsions Stabilized by Stimuli-Sensitive Microgels: Emulsions with Special Non-Pickering Properties. Langmuir **2012,** 28 (50), 17218-17229.

16.   Lyon, L. A.; Fernandez-Nieves, A., The Polymer/Colloid Duality of Microgel Suspensions. Annual Review of Physical Chemistry **2012,** 63 (1), 25-43.

17.   Deshmukh, O. S.; van den Ende, D.; Stuart, M. C.; Mugele, F.; Duits, M. H. G., Hard and soft colloids at fluid interfaces: Adsorption, interactions, assembly & rheology. Advances in Colloid and Interface Science **2014,** In Press.

18.   Pelton, R., Temperature-sensitive aqueous microgels. Advances in Colloid and Interface Science **2000,** 85 (1), 1-33.

19.   Aveyard, R.; Binks, B. P.; Clint, J. H., Emulsions stabilised solely by colloidal particles. Advances in Colloid and Interface Science **2003,** 100, 503-546.

20.   Destribats, M.; Lapeyre, V.; Wolfs, M.; Sellier, E.; Leal-Calderon, F.; Ravaine, V.; Schmitt, V., Soft microgels as Pickering emulsion stabilisers: role of particle deformability. Soft Matter **2011,** 7 (17), 7689-7698.

21.   Geisel, K.; Isa, L.; Richtering, W., Unraveling the 3D Localization and Deformation of Responsive Microgels at Oil/Water Interfaces: A Step Forward in Understanding Soft Emulsion Stabilizers. Langmuir **2012,** 28 (45), 15770-15776.

22.   Brugger, B.; Vermant, J.; Richtering, W., Interfacial layers of stimuli-responsive poly-(N-isopropylacrylamide-co-methacrylicacid) (PNIPAM-co-MAA) microgels characterized by

interfacial rheology and compression isotherms. Physical Chemistry Chemical Physics **2010,** 12 (43), 14573-14578.

23. Cohin, Y.; Fisson, M.; Jourde, K.; Fuller, G. G.; Sanson, N.; Talini, L.; Monteux, C., Tracking the interfacial dynamics of PNiPAM soft microgels particles adsorbed at the air-water interface and in thin liquid films. Rheologica Acta **2013,** 52 (5), 445-454.

24. Hellweg, T.; Dewhurst, C. D.; Eimer, W.; Kratz, K., PNIPAM-co-polystyrene Core−Shell Microgels: Structure, Swelling Behavior, and Crystallization. Langmuir **2004,** 20 (11), 4330-4335.

25. Ohshima, H., Electrokinetics of soft particles. Colloid and Polymer Science **2007,** 285 (13), 1411-1421.

26. Berne, B. J.; Pecora, R., Dynamic Light Scattering: With Applications to Chemistry, Biology, and Physics. Dover Publications: New York, 2000.

27. Adamson, A. W.; Gast, A. P., Physical Chemistry of Surfaces. 6th ed.; Wiley-Interscience: Canada, 1997.

28. Li, Z.; Geisel, K.; Richtering, W.; Ngai, T., Poly(N-isopropylacrylamide) microgels at the oil-water interface: adsorption kinetics. Soft Matter **2013,** 9 (41), 9939-9946.

29. Harbottle, D.; Chen, Q.; Moorthy, K.; Wang, L.; Xu, S.; Liu, Q.; Sjoblom, J.; Xu, Z., Problematic Stabilizing Films in Petroleum Emulsions: Shear Rheological Response of Viscoelastic Asphaltene Films and the Effect on Drop Coalescence. Langmuir **2014,** 30 (23), 6730-6738.

30. Vandebril, S.; Franck, A.; Fuller, G. G.; Moldenaers, P.; Vermant, J., A double wall-ring geometry for interfacial shear rheometry. Rheologica Acta **2010,** 49 (2), 131-144.

31.   Stieger, M.; Richtering, W.; Pedersen, J. S.; Lindner, P., Small-angle neutron scattering study of structural changes in temperature sensitive microgel colloids. Journal of Chemical Physics **2004,** 120 (13), 6197-6206.

32.   Daly, E.; Saunders, B. R., Temperature-dependent electrophoretic mobility and hydrodynamic radius measurements of poly(N-isopropylacrylamide) microgel particles: structural insights. Physical Chemistry Chemical Physics **2000,** 2 (14), 3187-3193.

33.   Kim, J. H.; Ballauff, M., The volume transition in thermosensitive core-shell latex particles containing charged groups. Colloid and Polymer Science **1999,** 277 (12), 1210-1214.

34.   Monteillet, H.; Workamp, M.; Appel, J.; Kleijn, J. M.; Leermakers, F. A. M.; Sprakel, J., Ultrastrong Anchoring Yet Barrier-Free Adsorption of Composite Microgels at Liquid Interfaces. Advanced Materials Interfaces **2014,** 1 (7), n/a-n/a.

35.   Zhang, J.; Pelton, R., Poly(N-isopropylacrylamide) at the Air/Water Interface. Langmuir **1996,** 12 (10), 2611-2612.

36.   Schild, H. G., POLY (N-ISOPROPYLACRYLAMIDE) - EXPERIMENT, THEORY AND APPLICATION. Prog. Polym. Sci. **1992,** 17 (2), 163-249.

37.   Du, K.; Glogowski, E.; Emrick, T.; Russell, T. P.; Dinsmore, A. D., Adsorption Energy of Nano- and Microparticles at Liquid−Liquid Interfaces. Langmuir **2010,** 26 (15), 12518-12522.

38.   Kutuzov, S.; He, J.; Tangirala, R.; Emrick, T.; Russell, T. P.; Boker, A., On the kinetics of nanoparticle self-assembly at liquid/liquid interfaces. Physical Chemistry Chemical Physics **2007,** 9 (48), 6351-6358.

39.   Ward, A. F. H.; Tordai, L., TIME-DEPENDENCE OF BOUNDARY TENSIONS OF SOLUTIONS .1. THE ROLE OF DIFFUSION IN TIME-EFFECTS. Journal of Chemical Physics **1946,** 14 (7), 453-461.

40. Tarimala, S.; Ranabothu, S. R.; Vernetti, J. P.; Dai, L. L., Mobility and in situ aggregation of charged microparticles at oil-water interfaces. Langmuir **2004,** 20 (13), 5171-5173.

41. Destribats, M.; Wolfs, M.; Pinaud, F.; Lapeyre, V.; Sellier, E.; Schmitt, V.; Ravaine, V., Pickering Emulsions Stabilized by Soft Microgels: Influence of the Emulsification Process on Particle Interfacial Organization and Emulsion Properties. Langmuir **2013,** 29 (40), 12367-12374.

42. Pawar, A. B.; Caggioni, M.; Ergun, R.; Hartel, R. W.; Spicer, P. T., Arrested coalescence in Pickering emulsions. Soft Matter **2011,** 7 (17), 7710-7716.

43. Arditty, S.; Whitby, C. P.; Binks, B. P.; Schmitt, V.; Leal-Calderon, F., Some general features of limited coalescence in solid-stabilised emulsions. Eur. Phys. J. E **2003,** 11 (3), 273-281.

44. Schmitt, V.; Ravaine, V., Surface compaction versus stretching in Pickering emulsions stabilised by microgels. Current Opinion in Colloid & Interface Science **2013,** 18 (6), 532-541.